JOURNAL OF GEOPHYSICAL RESEARCH, VOL. 92, NO. A4, PAGES 3293–3303, APRIL 1, 1987

Lightning-Induced Electron Precipitation Events Observed at $L \sim 2.4$ as Phase and Amplitude Perturbations on Subionospheric VLF Signals

U. S. INAN AND D. L. CARPENTER

STAR Laboratory, Stanford University, Stanford, California

Lightning-induced electron precipitation (LEP) events are studied using the Trimpi effect, in which the precipitation-induced ionization enhancements in the lower ionosphere (D region) give rise to rapid perturbations of subionospheric VLF signals. In 1983, the phase and amplitude of signals from the NPM transmitter in Hawaii (23.4 kHz) and the Omega transmitter in Argentina (12.9 kHz) were measured at Palmer, Antarctica ($L \sim 2.4$), together with the magnetospheric whistler background. The long baseline and over-sea great circle paths from these two sources make it possible for the observed perturbations to be interpreted using a single waveguide mode theory. Analytical expressions are used to relate the magnitude of the phase perturbations to differential changes in ionospheric reflection height along a segment of the propagation path. The predicted relationship between relative perturbation sizes on the two different signals is compared with measurements. From this information, the whistler-induced flux levels are inferred to be in the $10^{-4} - 10^{-2}$ erg cm^{-2} s^{-1} range and the precipitation regions are inferred to be roughly "circular" in shape, rather than elongated along L shells. Measured amplitude changes tended to be small ($\sim$ 0.5 dB) and negative, as expected from a single-mode theory, but the ratios of simultaneous amplitude and phase perturbations were slightly larger than the theory predicts, probably due to the effects of an additional mode(s). An assessment of the relative detectability of amplitude versus phase perturbations favors phase perturbations by $\sim$ 10 dB, irrespective of the detection scheme used.

1. INTRODUCTION

Precipitation of energetic radiation belt particles resulting from resonant interactions with electromagnetic waves is a subject of interest both as a loss process for the radiation belts and in terms of the resulting first-order perturbations of the nighttime lower ionosphere. The energetic particles are pitch angle scattered as a result of interactions with various kinds of magnetospheric waves, including whistlers generated by atmospheric lightning, spontaneous and triggered VLF emissions, and signals from man-made sources such as VLF transmitters and power lines. The energetic ($\sim$ 1-500 keV) electrons precipitated by the waves give rise to secondary ionization, optical emissions, X rays and heating in the ionosphere over the altitude range $\sim$ 80-200 km [*Helliwell et al.*, 1980; *Rosenberg et al.*, 1971].

Gyroresonant interaction with whistler waves generated by atmospheric lightning was put forth as a possible loss mechanism for trapped particles shortly after the discovery of the radiation belts [*Dungey*, 1963]. Recent experimental findings on whistler-induced precipitation, including indirect ground-based and direct satellite and rocket-based observations [*Helliwell et al.*, 1973; *Rycroft*, 1973; *Voss et al.*, 1984; *Goldberg et al.*, 1985], have renewed interest in this mechanism for coupling lightning and thunderstorms in the atmosphere to the trapped radiation in the earth's magnetosphere. As illustrated in Figure 1, a particularly sensitive ground-based technique for detecting lightning-induced electron precipitation is based on the so-called Trimpi effect, in which phase and amplitude changes of subionospheric VLF/LF signals occur as the result of precipitation induced perturbations of the ionosphere [*Helliwell et al.*, 1973; *Lohrey and Kaiser*, 1979; *Carpenter et al.*, 1984]. Such signal perturbations typically consist of fast (< 1 s) phase changes of a few degrees or amplitude increases or decreases of $\sim$1-6 dB, followed by a 10- to 30-s recovery to preevent values. These perturbations are attributed to alterations in the earth-ionosphere waveguide mode structure caused by localized enhancements in D region ionization produced by precipitating electrons with > 50 keV energy [*Helliwell et al.*, 1973].

Recent observations have shown that Trimpi events can be commonly observed near $L = 2$ [*Carpenter and LaBelle*, 1982; *Leyser et al.*, 1984] as perturbations on signals in the VLF, LF, and MF frequency ranges (up to $\sim$ 800 kHz) [*Lohrey and Kaiser*, 1979; *Carpenter et al.*, 1984; *Inan et al.*, 1985]. Events have been observed in the northern as well as in the southern hemisphere [*Dingle and Carpenter*, 1981; *Kintner and LaBelle*, 1984]. X rays and photoemissions due to whistler-induced precipitation have been detected poleward of the plasmapause, at subauroral latitudes [*Rosenberg et al.*, 1971; *Helliwell et al.*, 1980], as have Trimpi events [*Carpenter et al.*, 1985; *Hurren et al.*, 1986]. However, the Trimpi effect is the only ground based technique by which wave-induced burst precipitation has been detected on field lines threading the relatively dense ionization of the plasmasphere.

The Trimpi effect is a manifestation of a number of physical phenomena, including (1) the whistler-particle interaction in the magnetosphere that results in the precipitation of particles, (2) the generation of secondary ionization at D region altitudes by the precipitating particles, and (3) the resulting effects of the perturbed ionosphere on subionospheric VLF propagation. Extended utilization of this technique for measurement of wave-induced precipitation effects can potentially provide increased understanding of each of these phenomena.

Paper number 6A8679.
0148-0227/87/006A-8679$05.00

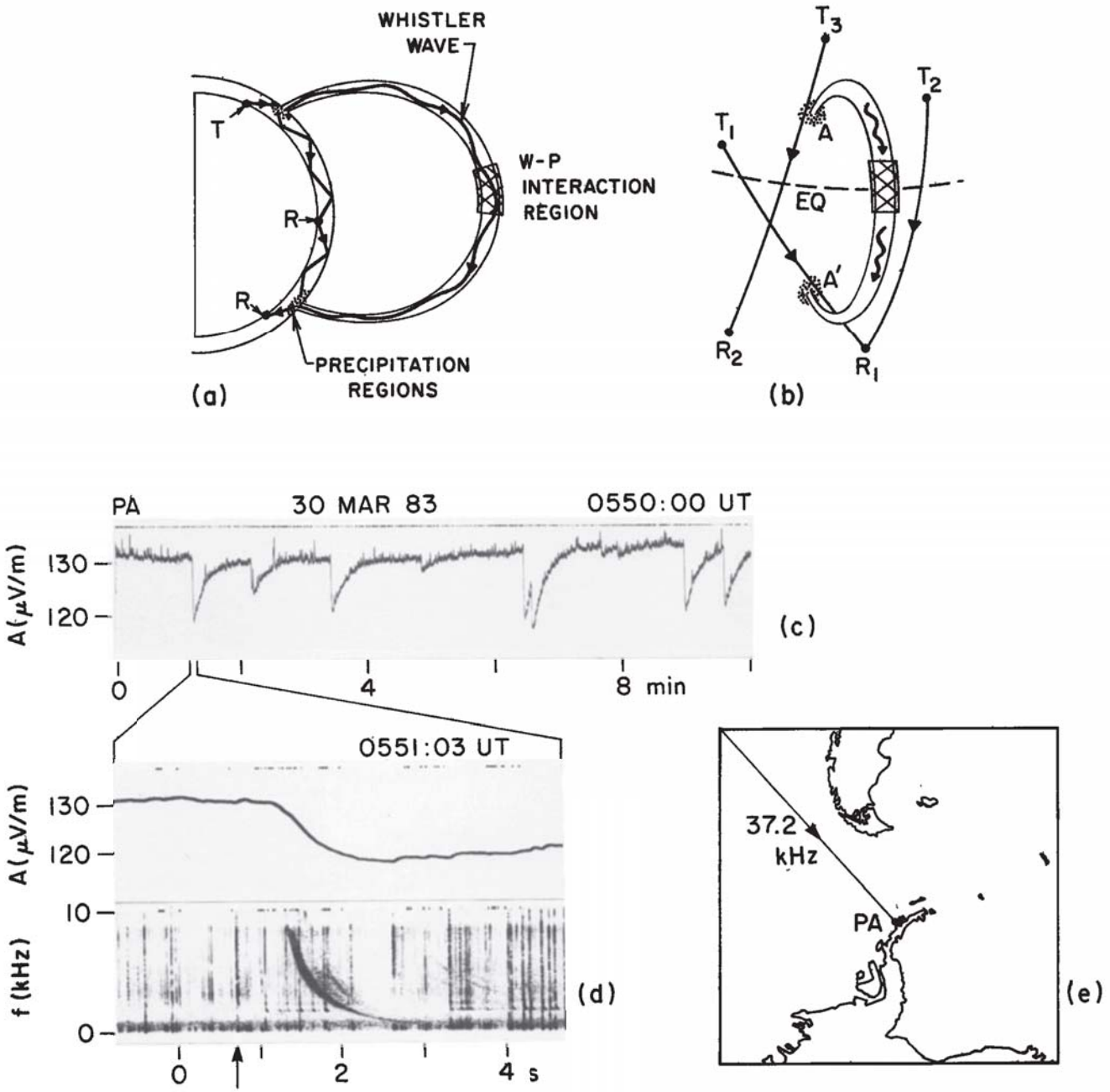

Fig. 1. Illustration of the detection of lightning-induced electron signal perturbations, i.e., the "Trimpi" effect; (*a*) meridional plane projection of the field line of propagation showing a whistler wave launched by a lightning discharge and a subionospheric VLF/LF/MF signal propagation path from a transmitter (T) to receivers (R), (*b*) a three-dimensional sketch showing the spatial relationship of the whistler mode duct and subionospheric signal paths between transmitters (T_1, T_2, T_3) and receivers (R_1, R_2) that cross the precipitation regions (A, A'), (*c*) chart recording showing "Trimpi" events as amplitude perturbations on a 37.2-kHz signal, originating in southern California, that was observed at Palmer Station (PA), Antarctica, (*d*) an expanded segment showing the 37.2-kHz perturbation in association with a magnetospheric whistler on a 0 to 10-kHz spectrum, with the arrow showing the estimated time of the lightning discharge that generated the whistler, and (*e*) map showing the location of Palmer and the great circle path from the 37.2-kHz signal source.

This paper is part of a continuing effort to extract quantitative information about ionospheric perturbations and incident fluxes from observed signal changes. In a previous paper, we presented an interpretive model of observed phase perturbations that included a single-mode subionospheric theory, a test particle model of the gyroresonant whistler-particle interaction in the magnetosphere, and estimates of ionospheric effects of precipitation fluxes [*Inan et al.*, 1985]. In the present paper we make more extensive use of single mode propagation theory, applying it to phase and amplitude data from two transmitters observed at Palmer Station, Antarctica. We then make preliminary inferences about the

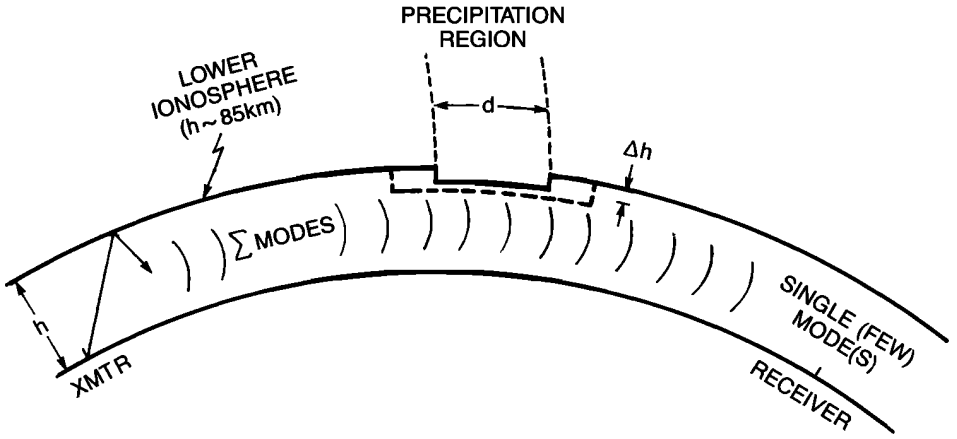

Fig. 2. Illustration of the single or few mode(s) model of earth-ionosphere waveguide propagation in the presence of localized perturbations.

characteristic shape of precipitation regions and the relative detectability of phase and amplitude changes, and also make further inferences about precipitation flux levels.

2. Quantitative Interpretation of Phase Trimpi Events

Quantitative interpretation of Trimpi events, for example to extract information on the associated precipitation flux levels, must be based on a model of the VLF/LF earth-ionosphere waveguide propagation in the presence of localized perturbations. The propagation of VLF/LF waves below the ionosphere is often analyzed in terms of a sum of modes traveling in the spherical waveguide formed by the earth's surface and the lower ionosphere. For realistic models of the lower ionosphere and ground conductivity, the mode analysis is complicated by the fact that each waveguide mode has a different attenuation rate along the propagation path [*Wait and Spies*, 1964], in addition to the differences that exist in the excitation efficiency at the source (usually a vertical antenna) for each mode. As discontinuities (such as sea-ground, sea-ice interfaces or localized ionospheric perturbations) are encountered along the signal path, mode conversion effects must also be taken into account [*Pappert and Snyder*, 1972]. In general the analysis of a given problem requires the use of a computer-based modeling approach [*Tolstoy et al.*, 1982, 1986], using average models of the lower ionopshere [*Ferguson*, 1980]. While such approaches are useful for obtaining quantitative results, the relative effects of different aspects of the problem are masked by the use of a complicated code. Thus, whenever possible, it is desirable to use simpler treatments that are based on certain limiting assumptions, but which nevertheless allow the development of a first-order analytical formulation of the problem.

Single-Mode Analysis of VLF Waveguide Propagation

One circumstance for which a simplified approach may be applicable is the case of the propagation of 10-to 25-kHz waves over a long all-sea path from the source to the receiver. In such a case, with no discontinuities along the propagation path, the "ground" consists of the seawater which can be treated as a perfect conductor. The lower ionosphere can be modeled either as a medium with either a sharp boundary or an exponential profile [*Wait*, 1959, 1962; *Wait and Spies*, 1964]. For such cases, and also assuming that the perturbed ionospheric region is distant (~200-500 km) from the receiver, the problem can be reduced to the analysis of single (or few) mode(s) that would be "dominant" at the receiver. As depicted in Figure 2, the precipitation region can then be decribed in terms of two parameters, Δh being the differential reduction of the lower ionospheric reflection height for the VLF signal, and d being the extent of the perturbed region along the propagation path.

For a sharply bounded isotropic ionosphere, and using the phase velocity expression given by *Wait* [1959], the phase change $\Delta\phi$ resulting from a localized, differential reduction

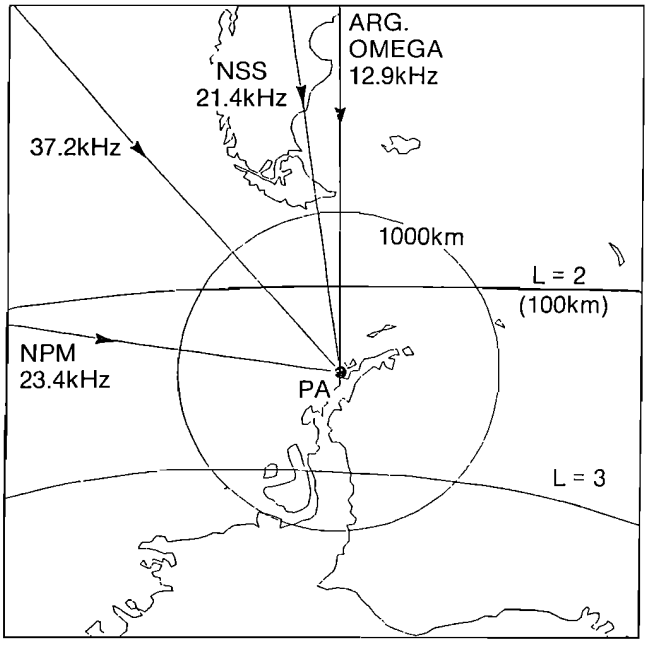

Fig. 3. Map showing various subionospheric signal paths observed at Palmer (PA) Station. The locations and operating frequencies of the various sources are given in Table 1. A circular contour of radius 1000 km centered at Palmer is shown for reference, as well as the loci of the feet of the $L = 2$ and $L = 3$ field lines at 100 km altitude.

Table 1. Transmitters Observed at Palmer Station

Transmitter	Location	Latitude	Longitude	Frequency, kHz
NSS	Maryland	39°N	76°W	21.4
NPM	Hawaii	21°N	158°W	23.4
LF (37.2 kHz)	California	35°N	117°W	37.2
Omega(ARG)	Argentina	43°S	65°W	12.9

Δh in the ionospheric reflection height can be expressed as

$$\frac{\Delta\phi}{d\Delta h} \simeq -\frac{2\pi f}{hc}\left[\frac{h}{2R_e} + C_n^2\right] \qquad C_n = \frac{(2n-1)\lambda}{4h} \quad (1)$$

where d is the length of the perturbed portion of the propagation path, n is of the order of the waveguide mode, R_e is the earth's radius, c is the speed of light, and f is the wave frequency. Note that the convention used for the enumeration of the waveguide modes is such that the nth-order mode refers to the waveguide mode TM_{0n}.

Application to NPM and Omega Argentina Signals Received at Palmer, Antarctica

Figure 3 shows the observation geometry at Palmer Station, Antarctica, where Stanford University conducted a program of Trimpi measurements during 1983. The loci of the L=2 and L=3 field lines at 100 km altitude are also shown for reference. The source locations and frequencies of some commonly monitored signals are given in Table 1. Most phase measurements were performed on signals from the NPM (23.4 kHz) and Omega Argentina (12.9 kHz) transmitters, propagating on great circle paths of lengths $\sim$ 12,335 km and $\sim$ 2400 km, respectively.

Arriving on long paths that are entirely sea-based, these two signals are particularly suited for single-mode analysis. Examples of whistler-associated phase and amplitude changes on the NPM signal are shown in Figures 4 and 5. Phase Trimpi events on the 12.9 kHz Omega Argentina signal were extensively discussed earlier [*Inan et al.*, 1985]. Experimental evidence that a single mode may be dominant in

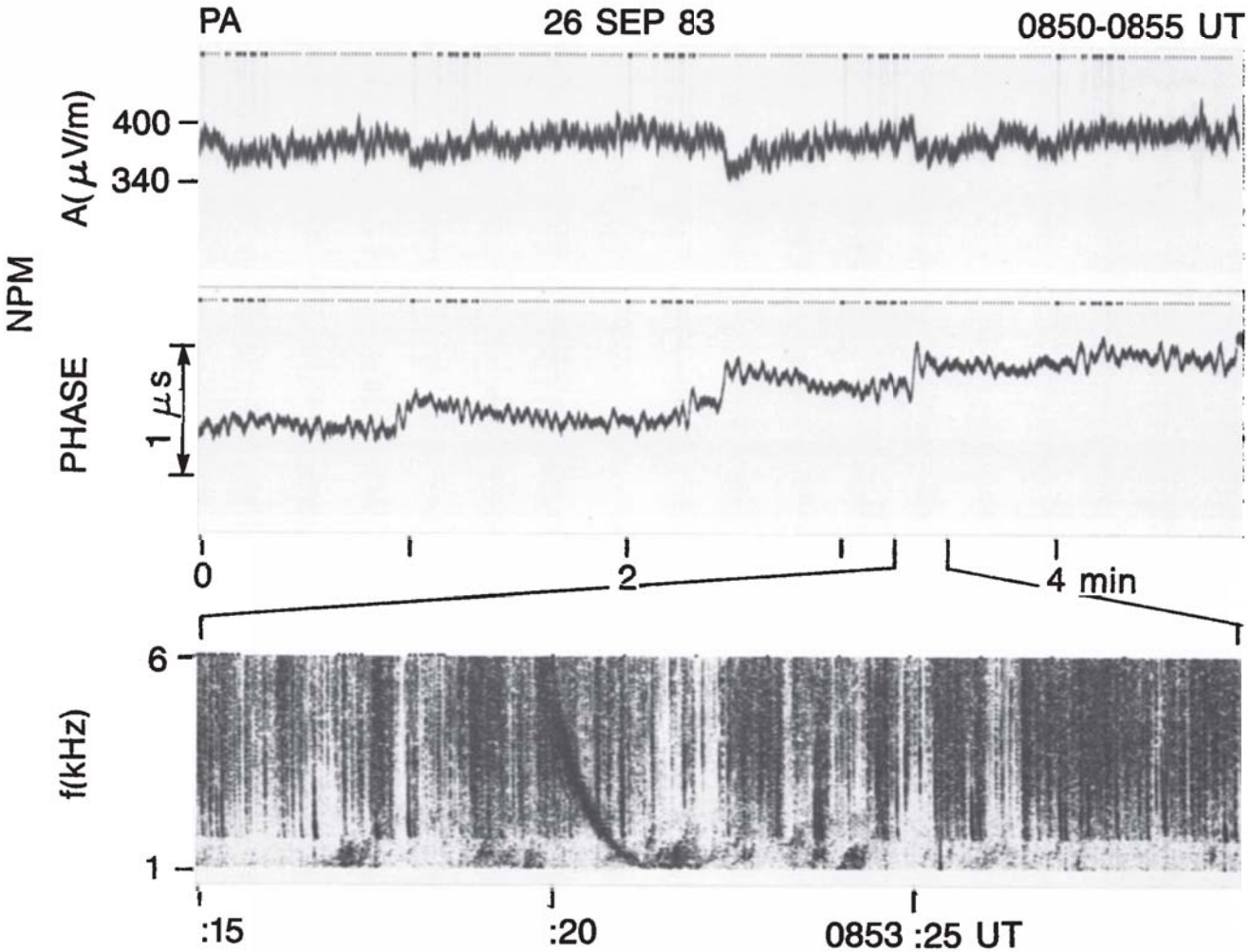

Fig. 4. Whistler-associated amplitude and phase perturbations (i.e., Trimpi events) observed at Palmer on the NPM signal. The top and middle panels respectively show the signal amplitude and phase; the bottom panel shows (on a time-expanded scale) the associated whistler on a 0 to 6 kHz frequency-time spectrum.

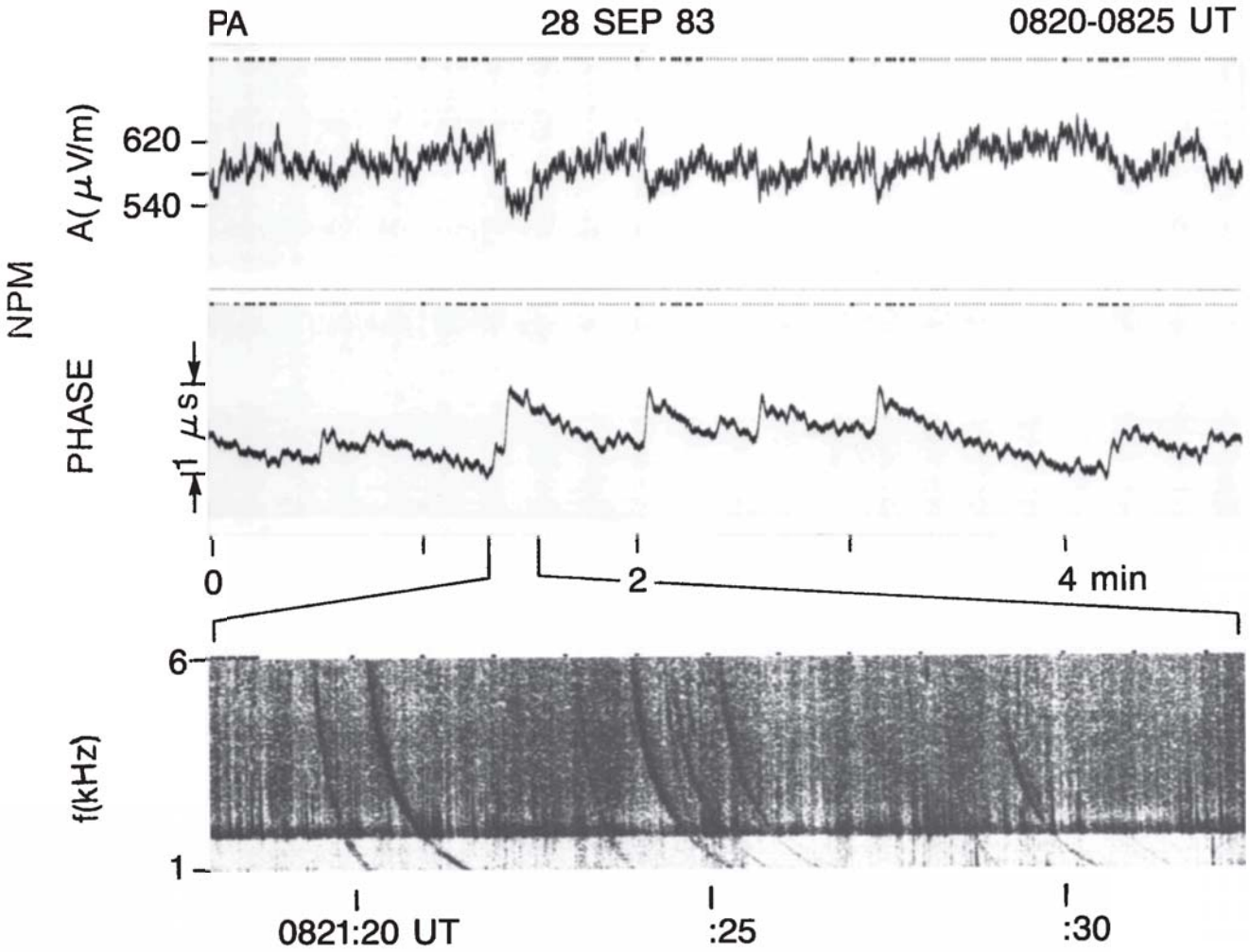

Fig. 5. Whistler-associated amplitude and phase perturbations observed at Palmer on the NPM signal. The top and middle panels show the signal amplitude and phase; the bottom panel shows (on a time-expanded scale) the associated whistler on a 0 to 6 kHz frequency-time spectrum.

the case of these two signals lies in the fact that an overwhelming fraction (> 95%) of all observed phase changes on NPM and Omega Argentina were positive as shown in Figure 4. Also, a similarly high fraction of observed amplitude changes on NPM involved decreases (Argentina Omega amplitude was not routinely recorded). These effects are consistent with the single mode model, since precipitation lowers the ionospheric reflection height, resulting in generally increased absorption and negative Δh. Further indication that the NPM signal as observed at Palmer consists mainly of a dominant single mode has been provided by the application of a detailed waveguide mode analysis model to the NPM-Palmer path [*Tolstoy et al.*, 1986].

Based on (1), negative phase changes may be attributed to interference between multiple modes. For example, phase perturbations on the 37.2 kHz LF signal at Palmer (see Figure 3 and Table 1) were found to vary regularly from positive to negative, consistent with the fact that in the LF frequency range, excitation factors and attenuation rates for lower order modes are comparable, so that a single mode analysis would not be expected to apply [*Davies*, 1966].

Using the results of *Wait and Spies* [1964] for the excitation factors and the attenuation rates of the two lowest-order

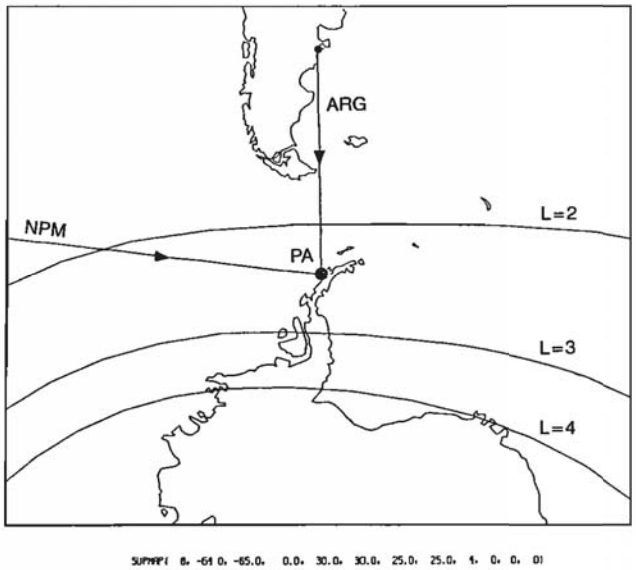

Fig. 6. Geometry of the great circle paths for the NPM and Omega Argentina signals observed at Palmer Station, Antarctica.

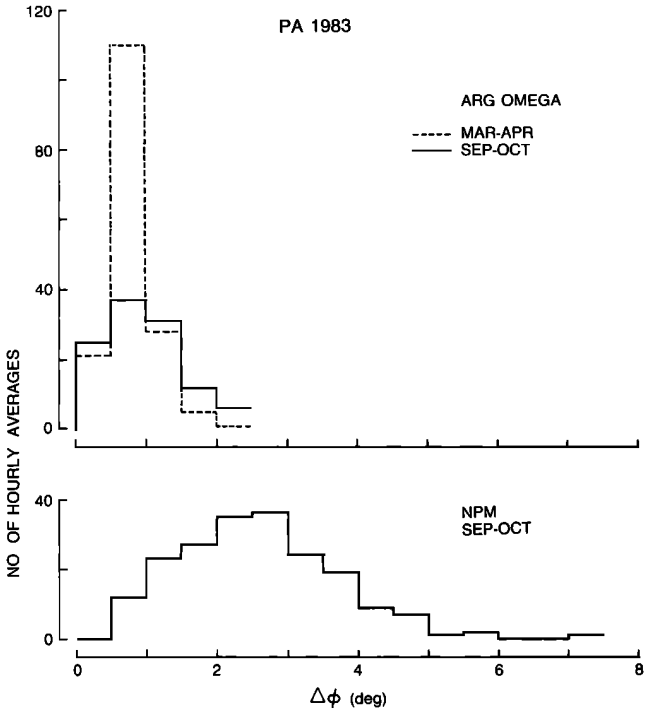

Fig. 7. Distribution of phase advances observed at Palmer on the NPM and Omega Argentina signals. Number of hourly averages in bins of 0.5° is shown. The distributions of individual perturbation sizes, not presented here, are similar to the hourly averages.

($n = 1, 2$) propagation modes (i.e., the waveguide modes TM_{01} and TM_{02}), we find that (1) for the 23.4 kHz-NPM signal observed at Palmer the second mode ($n = 2$) is dominant, being $\sim$ 9 dB larger than the first mode ($n = 1$), and (2) for the 12.9-kHz Omega Argentina (ARG) signal observed at Palmer the first mode ($n = 1$) is dominant, being $\sim$ 10 dB larger than the second mode ($n = 2$). (In our previous discussion of Argentina Omega phase at Palmer [*Inan et al.*, 1985], frequency dependent excitation factors were not taken into account and the second mode was assumed dominant. This assumption did not materially affect conclusions of that paper.) Accordingly, the expected phase changes for dominant modes, estimated on the single mode basis using (1), are

$$\frac{\Delta\phi}{d\Delta h} \simeq -2.1 \times 10^{-3} \quad \text{deg/(km)}^2 \quad \text{ARG } (n = 1) \quad (2a)$$

$$\frac{\Delta\phi}{d\Delta h} \simeq -6.4 \times 10^{-3} \quad \text{deg/(km)}^2 \quad \text{NPM } (n = 2) \quad (2b)$$

Based on this analysis, the phase changes on the NPM signal observed at Palmer Station are expected to be $\sim$ 3 times as large as those on the Omega Argentina signal, to the degree that $d\Delta h$ can be assumed to be the same for both signals. As discussed below, the differential height reduction Δh is a function of the precipitation flux level and energy spectrum, which can reasonably be expected to be similar in regions crossed by the two paths. However, due to the different orientations of the great circle paths with respect to L shells, the degree to which d is similar for both cases depends on the characteristic shapes of the precipitation regions. If, for example, the regions are on average elongated along L shells, the d corresponding to NPM can be expected to be a factor of $\sim$ 2.5 larger due to the grazing angle between the NPM-Palmer great circle path and the L shell contours, as illustrated in Figure 6. On the other hand, if the precipitation regions are roughly "circular" in shape, then the path orientation would not matter and the perturbed region size d would be expected to be similar for both the NPM and Omega Argentina signals.

Figure 7 shows the statistics of phase Trimpi events observed at Palmer on the NPM and Omega Argentina signals during September-October 1983. The distributions of hourly average values of $\Delta\phi$ are shown as a function of perturbation size $\Delta\phi$ in degrees. The distributions of individual perturbations, although not shown here, are quite similar to those of the hourly averages. We find that typical perturbation sizes for NPM lie in the range of 0.5°-6°, with values of 2°-3° being most common, while for Omega Argentina the corresponding ranges are 0°-2° and 0°-1.5°. Since the NPM changes are in general $\sim$ 3 times larger, the distributions of measured $\Delta\phi$ appear to be consistent with the estimates based on a single-mode analysis, provided that $d\Delta h$ is on the average similar for both signals. Within the context of the

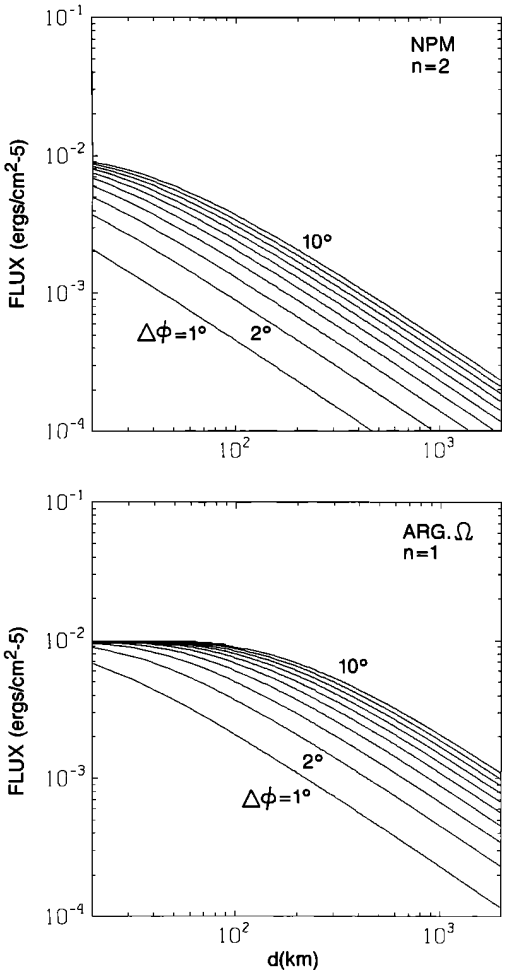

Fig. 8. (Top) Precipitating energy flux versus perturbed region size d for NPM phase changes of $\Delta\phi = 1°$-10°. The result shown was obtained using (1) and (3) for $n = 2$ and for the 23.4-kHz NPM signal, together with the ion pair production rate given by *Rees* [1969] and for an assumed precipitation pulse duration of $\sim$ 1 [*Inan et al.*, 1985]. (Bottom) Same for Omega Argentina (ARG) at 12.9 kHz and for n=1.

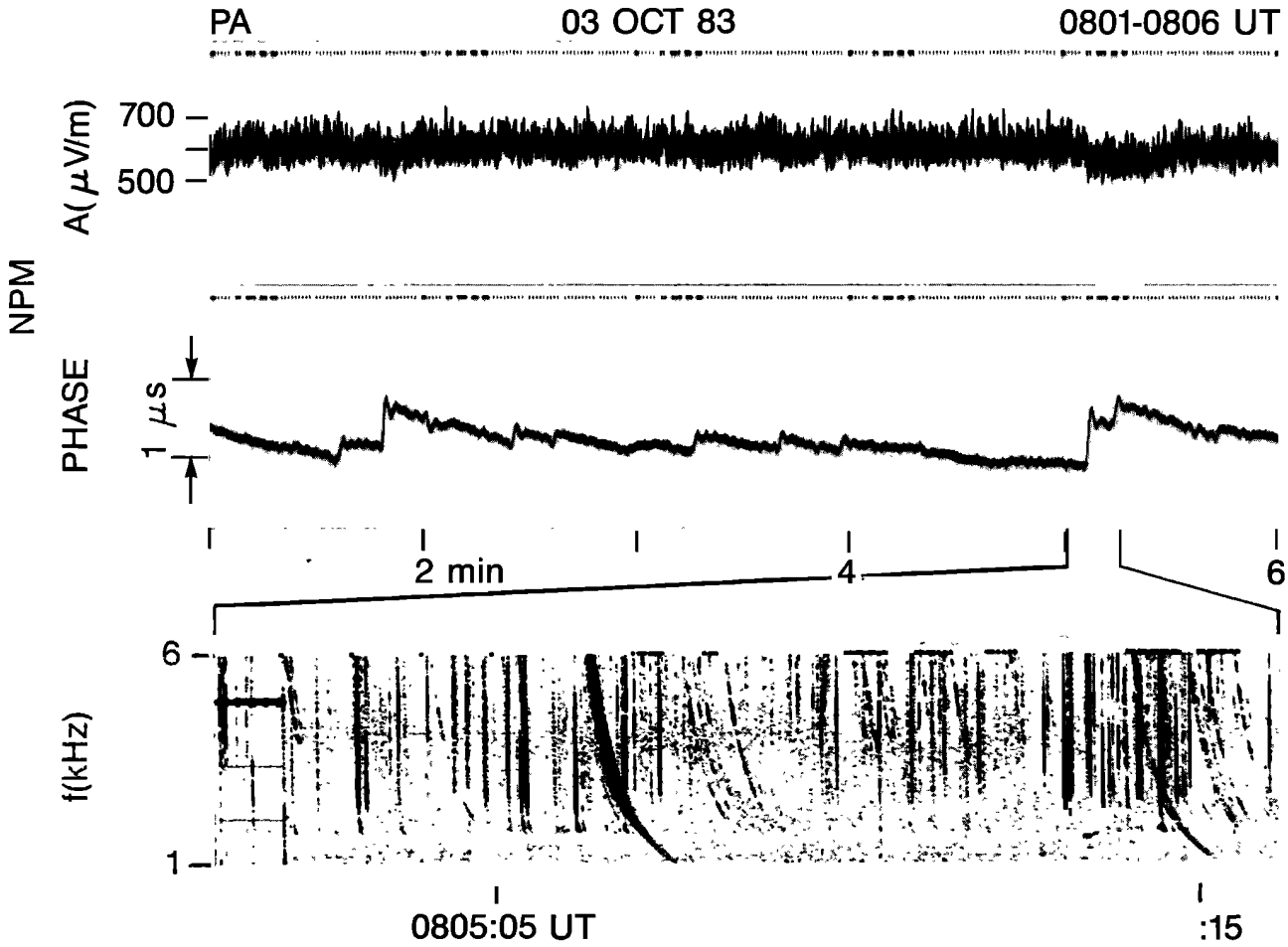

Fig. 9. Whistler-associated amplitude and phase perturbations observed at Palmer on the NPM signal. The top and middle panels show the signal amplitude and phase; the bottom panel shows (on a time-expanded scale) the associated whistler on a 0 to 6 kHz frequency-time spectrum. The example shown is representative of cases where sizable phase perturbations are not accompanied by clearly detectable amplitude perturbations.

single-mode theory, the data are therefore consistent with a "circular" precipitation region shape, rather than one that is elongated along geomagnetic longitude (i.e., L shells).

The indication that whistler-induced electron precipitation regions may exhibit circular shapes needs to be compared with the results of earlier theoretical work aimed at estimating spatial distribution of precipitation regions [*Inan et al.*, 1984]. This earlier work was limited to the consideration of precipitation induced by monochromatic VLF signals from ground-based VLF transmitters and it was concluded that precipitation regions would tend to be elongated along L shells. This follows mainly from the fact that for a fixed wave frequency, the wave-induced precipitation flux decreases rapidly with decreasing normalized frequency (i.e., f/f_{Heq}, where f_{Heq} is the equatorial gyrofrequency) and hence with decreasing geomagnetic latitude, while variations along L shells are mainly due to decreasing signal intensity in the earth-ionosphere waveguide with distance from the source. For the case of whistler-induced precipitation, a wider range of wave frequencies must be considered (typically 500 Hz to 6 kHz), so that interaction can occur at similar normalized frequencies (f/f_{Heq}) over a wider range of L shells. Furthermore, the theoretical prediction was based on an assumed plasmaspheric cold plasma density profile, a centered dipole model for the magnetic field, and "average" energetic electron distribution, and the assumed availability of continuous distribution of propagation paths (i.e., "ducts"). Thus, the above experimental finding of a tendency for precipitation regions to have "circular" shapes may be due to the combined influence of a number of factors.

Estimation of Precipitation Flux

Using an exponential ionospheric profile [*Wait and Spies*, 1964], the differential height reduction Δh can be related to a density enhancement ΔN_e. The latter can be related to the precipitation flux that produces it by using typical ion pair production rates at D region altitudes [*Rees*, 1969]. This scheme allows for a first-order interpretation of the observed phase changes ($\Delta\phi$) in terms of whistler-induced flux levels, if the perturbed region size d can be estimated [*Inan et al.*, 1985].

Direct experimental detection of d has so far not been possible, although *Carpenter and LaBelle* [1982] found preliminary evidence that the east-west extent of a perturbed region can be of order $\sim$ 100 km when there is a single correlated whistler component. Regarding the location of the precipitation regions, the preliminary empirical work of *Carpenter and LaBelle* [1982], based upon whistler information,

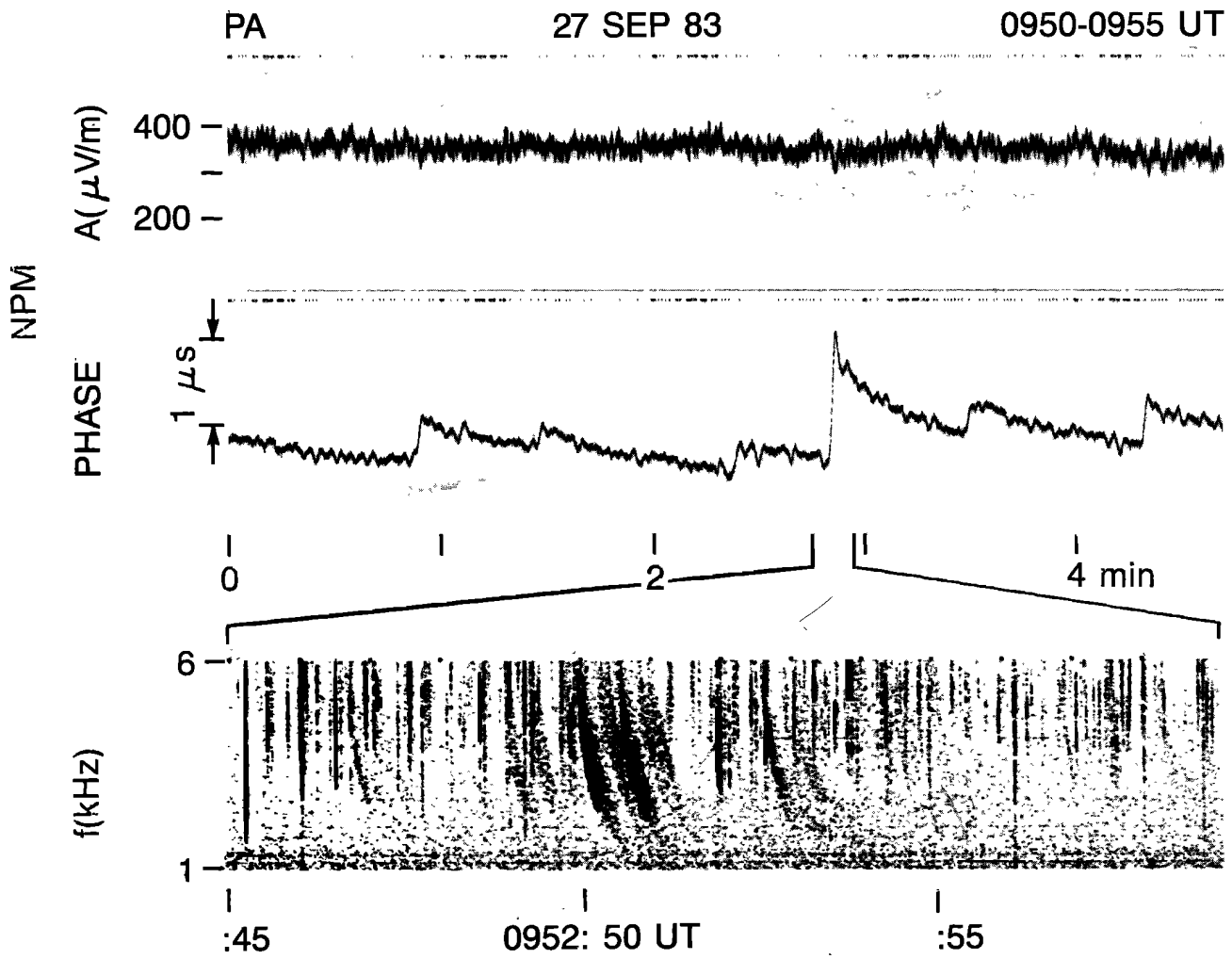

Fig. 10. Whistler-associated amplitude and phase perturbations observed at Palmer on the NPM signal. The top and middle panels show the signal amplitude and phase; the bottom panel shows (on a time-expanded scale) the associated whistler on a 0 to 6 kHz frequency-time spectrum. The example shown is representative of cases where sizable phase perturbations are not accompanied by clearly detectable amplitude perturbations.

and of *Leyser et al.* [1984], based upon information on terminator position, suggested that perturbations of predominantly north-south paths were usually centered less than ~ 400 km equatorward of Palmer, while perturbations of predominantly west-east paths could at times be located as far as 1000 to 2000 km from the station in a westerly direction. In the following, we determine the ranges of precipitation energy flux corresponding to a range of possible d values of 20-2000 km.

For a first-order calculation we assume exponential ionospheric profile given by [*Wait and Spies*, 1964]

$$N_e = 1.43 \times 10^7 e^{[-\beta h + (\beta - 0.15)(h + \Delta h)]}$$
$$\nu = 1.82 \times 10^{11} e^{[-0.15(h + \Delta h)]} \quad (3)$$

where h is the unperturbed reflection height (~ 85 km), N_e is the electron density in cm^{-3}, ν is the collision frequency, and the parameter β is taken to be $\simeq 0.5$ km^{-1}. Using an ion pair production rate at ~ 85 km altitude for ~ 150-keV particles of ~ 10^{-3} cm^{-3} s^{-1} per unit incident electron flux in cm^{-2} s^{-1} [*Rees*, 1969], and assuming precipitation pulse duration to be ~ 1 s [*Inan et al.*, 1985], the precipitating energy flux can be related to $\Delta\phi$ and d, through (1) and (3). A monoenergetic flux of particles at ~ 150 keV is used to represent precipitation consisting of particles in the ~ 40 to 250-keV range, since the ion pair production rate at ~ 85 km altitude is ~ 10^{-3} cm^{-3} over this energy range.

The results of this analysis for the dominant modes for NPM and Omega Argentina are shown in Figure 8, where the energy flux in ergs cm^{-2} s^{-1} is plotted against d (in km) for $\Delta\phi = 1°$-$10°$. We note that for reasonable perturbation region sizes of 100-2000 km, the $1°$-$6°$ phase changes observed on NPM (see Figure 13) correspond to a flux level of 10^{-4}-10^{-2} erg cm^{-2} s^{-1}. Furthermore, the $0°$-$2°$ phase changes for the Omega Argentina signal correspond to fluxes in the same range. This finding is consistent with recent satellite measurements of lightning-induced electron precipitation events in which the precipitating electron bursts were directly observed at ~ 200 km altitude [*Voss et al.*, 1984].

3. Interpretation of Amplitude Perturbations

Even for a single propagation mode, quantitative interpretation of amplitude perturbations cannot be based on a simple analytical expression similar to (1) above. This is mainly due to the fact that the computation of differential atten-

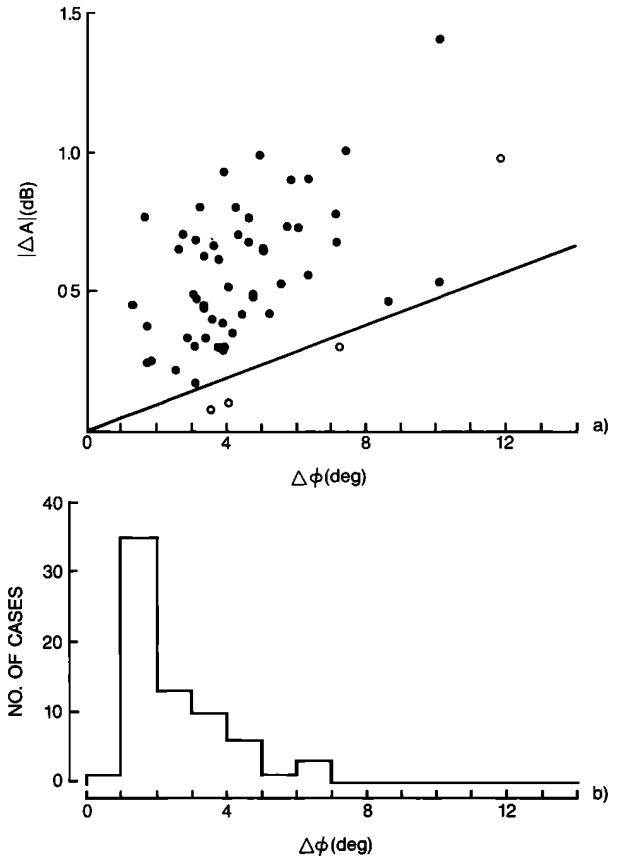

Fig. 11. Comparison of measured simultaneous amplitude (ΔA) and phase ($\Delta\phi$) perturbation sizes on the NPM signal observed at Palmer Station. The top panel shows data from 12 different periods during September-October 1983. In four of the periods fewer than three events could be scaled; these points are shown with open circles. The solid line shows the theoretically expected relationship of ΔA and $\Delta\phi$ as given by (6). The bottom panel shows a histogram of detectable phase changes for which any corresponding amplitude perturbations were below the noise level (typically ~ 0.3 dB) for recognition on the records.

uation (ΔA) due to a localized reflection height change of Δh must take into account the complete field configuration near the perturbation, using an imperfectly reflecting ionosphere and also accounting for the earth's curvature. For the interpretation of the amplitude perturbations, we rely on available published results, based on numerical model calculations carried out for the case of propagation of different modes in a flat earth-ionosphere waveguide with perfectly conducting earth and a finitely conducting isotropic ionosphere [*Wait*, 1962]. These conditions represent a suitable idealization of VLF propagation over seawater for an undisturbed ionosphere, as was also discussed above. Effects such as the curvature of the earth and the magnetic field were discussed in other work [*Wait and Spies*, 1960] and can be accounted for separately.

Specifically for the case of the 23.4-kHz NPM signal, the attenuation rates given by *Wait and Spies* [1964] for the second mode ($n = 2$) and for unperturbed reflection heights of $h = 80$ and 90 km are respectively 3.8 and 2.8 dB per 1000 km. Assuming the attenuation rate to vary linearly with reflection height between 80 and 90 km, and also taking into account a factor of ~ 3 increase in attenuation due to earth curvature [*Wait and Spies*, 1960], the differential attenuation due to a reflection height change of Δh over a portion of the path of length d is estimated to be

$$\frac{\Delta A}{d\Delta h} \simeq 3 \times 10^{-4} \quad \text{dB/(km)}^2 \tag{4}$$

The phase and amplitude perturbation estimates given by (2b) and (4) provide an opportunity for comparison of the single-mode results with data independent of the two unknowns d and Δh, using simultaneous measurements of phase and amplitude perturbations on the same signal. Based on (2*b*) and (4), we have

$$\frac{\Delta A}{\Delta\phi} \simeq 0.048 \quad \text{dB/deg} \tag{5}$$

as the expected relationship between ΔA and $\Delta\phi$.

During September-October 1983, simultaneous amplitude and phase measurements were carried out on the the 23.4-kHz NPM signal observed at Palmer Station, Antarctica. Examples of events were shown in Figures 4 and 5; two additional examples are given in Figures 9 and 10, illustrating cases in which relatively large phase changes were observed in the absence of detectable changes in amplitude. It should be noted that the amplitude measurements were made using a receiver with a bandwidth of ~ 300 Hz centered at 23.4 kHz; the phase measurements were made with a phase receiver tracking the signal phase within a bandwidth of ~ 50 Hz. The smoother nature of the phase curve is due to the relatively slow (0.5-1.0 s) response of the phase locked loop system to rapid phase changes.

Figure 11*a* shows a comparison of the measured simultaneous amplitude (ΔA) and phase ($\Delta\phi$) perturbations on the NPM signal observed at Palmer Station during 12 different periods. Most amplitude perturbations were found to be < 1 dB, indicating that the NPM signal amplitude observed at Palmer is relatively insensitive to precipitation-induced irregularities. This is consistent with the prediction of *Tolstoy et al.* [1986], and is attributed to the predominantly single-mode nature of the NPM signal at Palmer. For four of the periods fewer than three events could be scaled; these results are shown with open circles. In Figure 11*b* we show a histogram of detectable phase changes for which any corresponding amplitude perturbations were below the noise level for recognition on the records. Figure 10 provides an illustration of several such cases. The distribution peaks in the lower range of $\Delta\phi$, but also extends well into the range where ΔA values were at various times detected. The solid line in Figure 11*a* corresponds to (5) above and represents the predicted relation between ΔA and $\Delta\phi$ based on a single-mode theory.

We see that the measured relationship between ΔA and $\Delta\phi$ is in disagreement with the predicted single-mode behavior, indicating either that the measured ΔA values are larger than those given by (4) or that $\Delta\phi$ are lower than those given by (5). The reason for this is not clear, although it may be a result of interference between the dominant $n = 2$ mode and the $n = 1$ mode, whose amplitude is estimated to be ~ 9 dB lower at Palmer. From (1) the normalized phase change for the case of the 23.4-kHz NPM signal observed at Palmer and for $n = 1$ is found to be $[\Delta\phi/d\Delta h] \simeq -2.7\times10^{-3}$ deg/(km)^2. Depending on the unperturbed phase relationship between the field components of the two modes, the presence of the first mode may result in a larger amplitude change for the total field vector and/or a lower phase change.

Relative Sensitivity of VLF Phase Versus Amplitude

Using the perturbation sizes for NPM as given by (2) and (4), we can assess the relative sensitivity to localized ionospheric perturbations of phase versus amplitude of an individual VLF waveguide mode. The problem of detection of the coherent VLF signal in the presence of noise can be treated as a standard case of sine wave plus additive, narrow-band, Gaussian noise [*Davenport and Root*, 1958], i.e.,

$$a(t)\cos 2\pi ft + n(t) \simeq A(t)\cos(2\pi ft - \phi(t)) \qquad (6)$$

where $n(t)$ is a zero-mean, narrow-band Gaussian random process with a variance of σ_n^2.

For relatively large signal-to-noise ratios of $r = a/\sigma_n > 10$ (i.e., > 20 dB), the signal amplitude $A(t)$ is a Gaussian random variable with mean a and standard deviation σ_n, whereas the phase $\phi(t)$ is a Gaussian random variable with zero mean and standard deviation σ_n/a [*Davenport and Root*, 1958]. Based on this, and assuming a detectability threshold of one standard deviation from the mean, "detectable" phase and amplitude changes can be expressed in terms of r as

$$\Delta A \simeq 20\log[\frac{(r-1)}{r}] \text{ dB} \qquad \Delta\phi \simeq \frac{180}{\pi r} \text{ deg} \qquad (7)$$

To determine the relative sensitivity of phase and amplitude changes in response to a given ionospheric perturbation, the above "detectable" levels must be compared with the results given in (2b) and (4) that are based on the physics of the problem. As an example, for $r = 100$ (i.e., 40 dB), (7) gives $\Delta\phi = 0.57°$ and $\Delta A = -0.087$ dB. According to (2b), 0.57° corresponds to $| d\Delta h | \simeq 89$ km^2, whereas (4) gives $| d\Delta h | \simeq 290$ km^2 for an amplitude change of −0.087 dB. Thus, a "detectable" amplitude change requires a ~ 3.3 times larger ionospheric perturbation (either larger Δh or d or both) than a "detectable" phase change. Expressed in a different way, to detect an amplitude perturbation for the case of $| d\Delta h | \simeq 89$ km^2 would require a signal-to-noise ratio of $r = 325$ (or ~50 dB). Thus, in this case, the phase response is ~ 10 dB more sensitive than the amplitude response.

4. Summary and Conclusions

Whistler-associated VLF phase perturbations (i.e., phase Trimpi events) observed at Palmer Station, Antarctica, have been interpreted quantitatively to extract preliminary information about precipitation flux intensity and spatial distribution. For long, sea-based propagation paths, a simple, single-mode analysis of earth-ionosphere waveguide propagation appears to be usable for preliminary interpretation of the observed phase changes $\Delta\phi$ in terms of the differential reduction in ionospheric reflection height Δh and the extent of the perturbed region d. Results are consistent with precipitation region(s) that are roughly circular rather than substantially elongated along L shells. The whistler-induced energy fluxes that correspond to the observed phase changes are estimated to be of order $10^{-4} - 10^{-2}$ erg cm^{-2} s^{-1}, consistent with recent satellite observations. Measured amplitude changes tend to be small (~ 0.5 dB) and negative, as expected from a single mode theory, but the ratios of simultaneous amplitude and phase perturbations are slightly larger than the theory predicts, probably due to to the effects of an additional mode(s). An assessment of the relative detectability of amplitude versus phase perturbations favors phase perturbations by ~ 10 dB, irrespective of the detection scheme used.

Important questions regarding the spatial distribution of precipitation region(s) remain unanswered; more realistic models of the propagation and its perturbation, such as off-great-circle locations, as well as new experiments, are needed as part of continuing efforts to extract quantitative information concerning lightning-induced precipitation phenomena using the Trimpi technique. For future measurement, it seems clear that phase measurement are likely to be increasingly useful, since the response of the signal phase to a given ionospheric perturbation can be significantly more sensitive than is the amplitude.

Acknowledgments. We acknowledge useful discussions with our colleagues at STAR Laboratory, in particular with R. A. Helliwell. We thank J. Katsufrakis for his excellent management of the Stanford field programs, J. Yarbrough for his help in processing the spectrograms, P. Pecen for preparation of the Figures, and K. Fletcher for typing the manuscript. The research was supported by the Division of Atmospheric Sciences of the National Science Foundation (NSF) under grant ATM-8415464, and also by the Division of Polar Programs of NSF under grants DPP-82-17820 and DPP-80-22282.

The Editor thanks A. Tolstoy and a second referee for their assistance in evaluating this paper.

References

Carpenter, D. L., and J. W. LaBelle, A study of whistlers correlated with bursts of electron precipitation near $L = 2$, *J. Geophys. Res., 87*, 4427, 1982.

Carpenter, D. L., U. S. Inan, M. L. Trimpi, R. A. Helliwell, and J. P. Katsufrakis, Perturbations of subionospheric LF and MF signals due to whistler-induced electron precipitation bursts, *J. Geophys. Res., 89*, 9857, 1984.

Carpenter, D. L., U. S. Inan, E. V. Paschal, and A. J. Smith, A new VLF method for studying burst precipitation near the plasmapause, *J. Geophys. Res., 90*, 4383, 1985.

Davenport, W. P., and W. L. Root, *Random Signals and Noise*, McGraw-Hill, New York, 1958.

Davies, K., *Ionospheric Radio Propagation*, Dover, New York, 1966.

Dingle, B., and D. L. Carpenter, Electron precipitation induced by VLF noise bursts at the plasmapause and detected at conjugate ground stations, *J. Geophys. Res., 86*, 4597, 1981.

Dungey, J. W., Loss of Van Allen electrons due to whistlers, *Planet. Space Sci., 11*, 591, 1963.

Ferguson, J. A., Ionospheric profiles for predicting nighttime VLF/LF propagation, *Tech. Rep. 530*, Naval Ocean Systems Command, San Diego, Calif., 1980.

Goldberg, R. A., J. R. Barcus, L. C. Hale, and S. A. Curtis, Direct observation of magnetospheric electron precipitation stimulated by lightning, *J. Atmos. Terr. Phys., 48*, 293, 1986.

Helliwell, R. A., J. P. Katsufrakis, and M. L. Trimpi, Whistler-induced amplitude perturbation in VLF propagation, *J. Geophys. Res., 78*, 4679, 1973.

Helliwell, R. A., S. B. Mende, J. H. Doolittle, W. C. Armstrong, and D. L. Carpenter, Correlations between λ4278 optical emissions and VLF wave events observed at $L \simeq 4$ in the Antarctic, *J. Geophys. Res., 85*, 3376, 1980.

Hurren, P. J., A. J. Smith, D. L. Carpenter, and U. S. Inan, Burst precipitation-induced perturbations on multiple VLF propagation paths in Antarctica, *Ann. Geophys., Gauthier Villars*, in press, 1986.

Inan, U. S., H. C. Chang, and R. A. Helliwell, Electron precipitation zones around major ground-based VLF signal sources, *J. Geophys. Res., 89*, 2891, 1984.

Inan, U. S., D. L. Carpenter, R. A. Helliwell, and J. P. Katsufrakis, Subionospheric VLF/LF phase perturbations produced by lightning-whistler induced particle precipitation, *J. Geophys. Res., 90*, 7457, 1985.

Kintner, P. M., and J. W. LaBelle, Very short path length Trimpi observations, *Eos Trans. AGU, 65*, 1059, 1984.

Leyser, T., U. S. Inan, D. L. Carpenter, and M. L. Trimpi, Diurnal variation of burst precipitation effects on subionospheric VLF/LF signal propagation near $L = 2$, *J. Geophys. Res., 89*, 9139, 1984.

Lohrey, B., and A. B. Kaiser, Whistler-induced anomalies in VLF propagation, *J. Geophys. Res., 84*, 5121, 1979.

Pappert, R. A., and F. P. Snyder, Some results of a mode-conversion program for VLF, *Radio Sci., 7*, 913, 1972.

Rees, M. H., Auroral electrons, *Space Sci. Rev., 10*, 413, 1969.

Rosenberg, T. J., R. A. Helliwell, and J. P. Katsufrakis; Electron precipitation associated with discrete very-low-frequency emissions, *J. Geophys. Res., 76*, 8445, 1971.

Rycroft, M. J., Enhanced energetic electron intensities at 100 km altitude and a whistler propagating through the plasmapause, *Planet. Space Sci., 21*, 239, 1973.

Tolstoy, A., The influence of localized precipitation-induced D-region ionization enhancements on subionospheric VLF propagation, Ph.D. thesis, Univ. of Md., College Park, 1983.

Tolstoy, A., T. J. Rosenberg, and D. L. Carpenter, The influence of localized precipitation-induced D region ionization enhancements on subionospheric VLF propagation, *Geophys. Res. Lett., 9*, 563, 1982.

Tolstoy, A., T. J. Rosenberg, U. S. Inan, and D. L. Carpenter, Model predictions of subionospheric VLF signal perturbations resulting from localized, electron precipitation induced ionization enhancement regions, *J. Geophys. Res.,91*, 13,473, 1986.

Voss, H. D., W. L. Imhof, J. Mobilia, E. E. Gaines, M. Walt, U. S. Inan, R. A. Helliwell, D. L. Carpenter, J. P. Katsufrakis, H. C. Chang, Lightning induced electron precipitation, *Nature, 312*, 740, 1984.

Wait, J. R., Diurnal change of ionospheric heights deduced from phase velocity measurements at VLF, *Proc. IRE*, 998, 1959.

Wait, J. R., *Electromagnetic Waves in Stratified Media*, Pergamon, New York, 1962.

Wait, J. R., and K. Spies, Influence of earth curvature and terrestrial magnetic field on VLF propagation, *J. Geophys. Res., 65*, 2325, 1960.

Wait, J. R., and K. P. Spies, Characteristics of the earth-ionosphere waveguide for VLF radio waves, *NBS Tech. Note 300*, 1964.

D. L. Carpenter and U. S. Inan, STAR Laboratory, Department of Electrical Engineering/SEL, Durand 324, Stanford University, Stanford, CA 94305.

(Received August 4, 1986;
revised September 30, 1986;
accepted November 17, 1986.)